

## Synthesis and Structure–Activity Relationships of a New Model of Arylpiperazines. 6. Study of the 5-HT<sub>1A</sub>/α<sub>1</sub>-Adrenergic Receptor Affinity by Classical Hansch Analysis, Artificial Neural Networks, and Computational Simulation of Ligand Recognition<sup>†</sup>

María L. López-Rodríguez,<sup>\*,§</sup> M. José Morcillo,<sup>‡</sup> Esther Fernández,<sup>§</sup> M. Luisa Rosado,<sup>§</sup> Leonardo Pardo,<sup>⊥</sup> and Klaus-Jürgen Schaper<sup>#</sup>

Departamento de Química Orgánica I, Facultad de Ciencias Químicas, Universidad Complutense, 28040 Madrid, Spain, Facultad de Ciencias, Universidad Nacional de Educación a Distancia, 28040 Madrid, Spain, Laboratori de Medicina Computacional, Unitat de Bioestadística, Facultat de Medicina, Universitat Autònoma de Barcelona, 08193 Bellaterra, Spain, and Research Center Borstel, D-23845 Borstel, Germany

Received February 23, 2000

A classical quantitative structure–activity relationship (Hansch) study and artificial neural networks (ANNs) have been applied to a training set of 32 substituted phenylpiperazines with affinity for 5-HT<sub>1A</sub> and α<sub>1</sub>-adrenergic receptors, to evaluate the structural requirements that are responsible for 5-HT<sub>1A</sub>/α<sub>1</sub> selectivity. The resulting models provide a significant correlation of electronic, steric, and hydrophobic parameters with the biological affinities. Although the derived linear Hansch correlations give good statistics and acceptable predictions, the introduction of nonlinear relationships in the analysis gives more solid models and more accurate predictions. In the ANN models on the basis of the obtained 3D plots, the 5-HT<sub>1A</sub> affinity has a nonlinear dependence on  $F$ ,  $V_o$ ,  $V_m$ , and  $\pi_o$ , although the nonlinear relationship is not far from a planar one. The α<sub>1</sub>-adrenergic receptor affinity has a clear nonlinear dependence on  $F$ ,  $V_o$ ,  $V_m$ ,  $\pi_o$ , and  $\pi_m$ . A comparison of both analyses gives an additional understanding for 5-HT<sub>1A</sub>/α<sub>1</sub> selectivity: (a) high  $F$  values increase the binding affinity for 5-HT<sub>1A</sub> receptors and decrease the affinity for α<sub>1</sub> sites; (b) the hydrophobicity at the *meta*-position has only influence for the α<sub>1</sub>-adrenergic receptor; (c) the *meta*-position seems to be implicated in the 5-HT<sub>1A</sub>/α<sub>1</sub> selectivity. While the 5-HT<sub>1A</sub> receptor is able to accommodate bulky substituents in the region of its active site, the steric requirements of the α<sub>1</sub>-adrenergic receptor at this position are more restricted. This information was used for the design of the new ligand EF-7412 (**33**) (5-HT<sub>1A</sub>:  $K_i^{\text{exptl}} = 27$  nM, α<sub>1</sub>:  $K_i^{\text{exptl}} > 1000$  nM; 5-HT<sub>1A</sub>:  $K_i^{\text{pred ANN}} = 36$  nM, α<sub>1</sub>:  $K_i^{\text{pred ANN}} = 2745$  nM) which was characterized as an antagonist *in vivo* in pre- and postsynaptic 5-HT<sub>1A</sub>R sites. Computational simulations of the complex between EF-7412 (**33**) and a 3D model of the transmembrane domain of the 5-HT<sub>1A</sub> receptor allowed us to define the molecular details of the ligand–receptor interaction that includes: (i) the ionic interaction between the protonated amine of the ligand and Asp 3.32; (ii) the hydrogen bonds between the *m*-NHSO<sub>2</sub>Et group of the ligand and Asn 7.39; and the hydrogen bonds between the hydantoin moiety of the ligand and (iii) Thr 3.37, (iv) Ser 5.42, and (v) Thr 5.43. These QSAR and ANN results in combination with computational simulations of ligand recognition will be useful for the design of potent selective 5-HT<sub>1A</sub> ligands.

### Introduction

The formulation of quantitative structure–activity relationships (QSAR) is an important tool in the development of new agents because it can keep the number of synthesized and tested compounds to a minimum. Hansch<sup>1</sup> demonstrated that the biological activities of drug molecules can be correlated by a linear combination of the physicochemical parameters of the corresponding drug. However in the cases that biological activities do not vary in a linear manner with physico-

chemical parameters, cross-product terms must be included in the regression analysis. This adds complexity to data analysis and interpretation. During the past years artificial neural networks (ANNs) have been applied successfully in the QSAR field.<sup>2,3</sup> It has been demonstrated that this new technique is often superior to the traditional Hansch approach, providing more accurate predictions. The advantage of ANNs is that with the presence of hidden layers, neural networks are implicitly able to perform nonlinear mapping of the physicochemical parameters to the corresponding biological activities.<sup>4</sup>

The preceding paper in this series describes the design and synthesis of a test series of 32 arylpiperazine derivatives with affinity for 5-HT<sub>1A</sub> and α<sub>1</sub>-adrenergic receptors. The wide range of receptor affinities of these

<sup>†</sup> Dedicated to Professor José Luis Soto on the occasion of his 70th birthday.

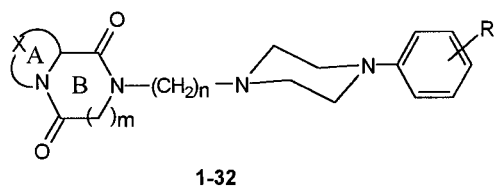
\* To whom correspondence should be addressed. Phone: 34-91-3944239. Fax: 34-91-3944103. E-mail: mluzlr@eucmax.sim.ucm.es.

<sup>§</sup> Universidad Complutense.

<sup>‡</sup> Universidad Nacional de Educación a Distancia.

<sup>⊥</sup> Universitat Autònoma de Barcelona.

<sup>#</sup> Research Center Borstel.



1-32

X =  $-(\text{CH}_2)_3-$ ,  $-(\text{CH}_2)_4-$ ;

m = 0, 1; n = 3, 4

R = *ortho* and *meta* positions (*o*-CH<sub>3</sub>, *o*-OCH<sub>3</sub>, *o*-OBu, *o*-COOPr  
*o*-CONHPr, *o*-CN, *m*-CF<sub>3</sub>, *m*-NH<sub>2</sub>, *m*-NHCOPr<sup>t</sup>, *m*-Br)

**Figure 1.** Compounds 1–32.

compounds, which is due to a rational choice of substituents, makes this material suitable for a QSAR investigation.

A classical Hansch regression analysis and ANNs were employed to sort out the structural requirements that are responsible for 5-HT<sub>1A</sub>/α<sub>1</sub> selectivity. This type of analysis leads to the identification and characterization of the physicochemical factors of the pharmacophore on which biological affinity and selectivity (5-HT<sub>1A</sub> vs α<sub>1</sub> affinity) are based. In the present paper we report the results of this study, which provided information for the design of the ligand EF-7412 (**33**) (5-HT<sub>1A</sub>: K<sub>i</sub> = 27 nM; α<sub>1</sub>: K<sub>i</sub> > 1000 nM).

The 5-HT<sub>1A</sub> receptor (5-HT<sub>1AR</sub>) belongs to the family of G protein-coupled receptors (GPCRs). Recently, the detailed 3D structure of bovine rhodopsin (RHO) was determined at 2.8 Å resolution.<sup>5</sup> This major breakthrough has confirmed that RHO and the RHO-like family of GPCRs are formed by seven antiparallel α-helical transmembrane domains connected by hydrophilic loops. The highly conserved motifs that characterize the RHO-like family of GPCRs are all located in the transmembrane region, which suggests a common transmembrane structure. In contrast the extracellular domain diverges in the GPCRs family.<sup>6</sup> Here we present the derivation, from the crystal structure of RHO,<sup>5</sup> of a computational model of the complex between EF-7412 (**33**) and the transmembrane domain of the 5-HT<sub>1AR</sub>. The computed model rests on the definition of the putative residues of the ligand-binding site guided by published results of modifications of GPCRs using methods of molecular biology. These insights obtained from classical Hansch analysis, ANNs, and computational simulations of ligand recognition can be used to guide the design of ligands with predetermined affinities and selectivity.

## Materials and Methods

**Data Set.** The training set of 32 phenylpiperazines substituted in the *ortho*- and *meta*-positions (Figure 1) was evaluated for in vitro 5-HT<sub>1A</sub> and α<sub>1</sub>-adrenergic receptor affinities by radioligand binding assays. The compounds were first tested at the fixed dose of 10<sup>-6</sup> M, and for those that in this prescreening process presented high activity (displacement of the radioligand ≥ 55%), the dose–response curves were determined. However, for the members of the series showing low activity (displacement < 55%) the binding constants were not determined. Nevertheless, low-activity compounds of a drug series allow the activity scale to be expanded. Obviously a broad range of activity data facilitates the recognition of QSAR relationships. The estimation of the IC<sub>50</sub> values for the compounds where

**Table 1.** 5-HT<sub>1A</sub> and α<sub>1</sub>-Adrenergic Receptor Binding Data<sup>a</sup>

compd	X	m	n	R	5-HT <sub>1A</sub>		α <sub>1</sub>	
					K <sub>i</sub> (nM) ±SEM <sup>b</sup>	pK <sub>i</sub> <sup>c</sup>	K <sub>i</sub> (nM) ±SEM <sup>b</sup>	pK <sub>i</sub> <sup>c</sup>
1	-(CH <sub>2</sub> ) <sub>3</sub> -	0	3	<i>o</i> -OBu	15 ± 2	7.82	6.4 ± 4.2	8.19
2	-(CH <sub>2</sub> ) <sub>3</sub> -	0	3	<i>o</i> -CONHPr	808	6.09	608	6.22
3	-(CH <sub>2</sub> ) <sub>3</sub> -	0	3	<i>m</i> -NH <sub>2</sub>	1182	5.93	393	6.41
4	-(CH <sub>2</sub> ) <sub>3</sub> -	0	3	<i>m</i> -Br	34 ± 9	7.47	25 ± 2	7.61
5	-(CH <sub>2</sub> ) <sub>4</sub> -	0	3	<i>o</i> -CH <sub>3</sub>	220 ± 2	6.66	5.7 ± 0.2	8.25
6	-(CH <sub>2</sub> ) <sub>4</sub> -	0	3	<i>o</i> -COOPr	46 ± 6	7.34	13 ± 1	7.89
7	-(CH <sub>2</sub> ) <sub>4</sub> -	0	3	<i>o</i> -CN	65 ± 12	7.19	8.2 ± 0.8	8.09
8	-(CH <sub>2</sub> ) <sub>4</sub> -	0	3	<i>m</i> -NHCOPr <sup>t</sup>	776	6.11	4430	5.35
9	-(CH <sub>2</sub> ) <sub>3</sub> -	1	3	<i>o</i> -CH <sub>3</sub>	48 ± 2	7.31	17 ± 1	7.76
10	-(CH <sub>2</sub> ) <sub>3</sub> -	1	3	<i>o</i> -COOPr	55 ± 3	7.26	12 ± 7	7.93
11	-(CH <sub>2</sub> ) <sub>3</sub> -	1	3	<i>o</i> -CN	27 ± 5	7.56	17 ± 3	7.76
12	-(CH <sub>2</sub> ) <sub>3</sub> -	1	3	<i>m</i> -NHCOPr <sup>t</sup>	266 ± 72	6.57	1440	5.84
13	-(CH <sub>2</sub> ) <sub>4</sub> -	1	3	<i>o</i> -OCH <sub>3</sub>	143 ± 8	6.84	29 ± 1	7.53
14	-(CH <sub>2</sub> ) <sub>4</sub> -	1	3	<i>o</i> -OBu	92 ± 15	7.04	13 ± 15	7.89
15	-(CH <sub>2</sub> ) <sub>4</sub> -	1	3	<i>o</i> -CONHPr	4614	5.34	811	6.09
16	-(CH <sub>2</sub> ) <sub>4</sub> -	1	3	<i>m</i> -CF <sub>3</sub>	179 ± 21	6.75	339 ± 3	6.47
17	-(CH <sub>2</sub> ) <sub>3</sub> -	0	4	<i>o</i> -CH <sub>3</sub>	16 ± 2	7.78	7.0 ± 2.1	8.15
18	-(CH <sub>2</sub> ) <sub>3</sub> -	0	4	<i>o</i> -COOPr	4.8 ± 1.4	8.32	41 ± 5	7.39
19	-(CH <sub>2</sub> ) <sub>3</sub> -	0	4	<i>o</i> -CN	4.0 ± 0.8	8.40	4.9 ± 1.4	8.31
20	-(CH <sub>2</sub> ) <sub>3</sub> -	0	4	<i>m</i> -NHCOPr <sup>t</sup>	193 ± 8	6.72	5425	5.27
21	-(CH <sub>2</sub> ) <sub>4</sub> -	0	4	<i>o</i> -OBu	2.2 ± 0.1	8.66	5.0 ± 0.3	8.30
22	-(CH <sub>2</sub> ) <sub>4</sub> -	0	4	<i>o</i> -CONHPr	378 ± 106	6.42	521	6.28
23	-(CH <sub>2</sub> ) <sub>4</sub> -	0	4	<i>m</i> -NH <sub>2</sub>	68 ± 18	7.17	231 ± 6	6.64
24	-(CH <sub>2</sub> ) <sub>4</sub> -	0	4	<i>m</i> -Br	5.4 ± 1.1	8.27	5.9 ± 0.3	8.23
25	-(CH <sub>2</sub> ) <sub>3</sub> -	1	4	<i>o</i> -OCH <sub>3</sub>	12 ± 1	7.92	25 ± 1	7.59
26	-(CH <sub>2</sub> ) <sub>3</sub> -	1	4	<i>o</i> -OBu	8.7 ± 1.1	8.06	10.5 ± 8.6	7.98
27	-(CH <sub>2</sub> ) <sub>3</sub> -	1	4	<i>o</i> -CONHPr	1232	5.91	1354	5.87
28	-(CH <sub>2</sub> ) <sub>3</sub> -	1	4	<i>m</i> -CF <sub>3</sub>	5.5 ± 0.6	8.26	72 ± 11	7.14
29	-(CH <sub>2</sub> ) <sub>4</sub> -	1	4	<i>o</i> -CH <sub>3</sub>	32 ± 8	7.50	27 ± 2	7.56
30	-(CH <sub>2</sub> ) <sub>4</sub> -	1	4	<i>o</i> -COOPr	28 ± 6	7.55	392 ± 33	6.41
31	-(CH <sub>2</sub> ) <sub>4</sub> -	1	4	<i>o</i> -CN	15 ± 1	7.82	30 ± 5	7.52
32	-(CH <sub>2</sub> ) <sub>4</sub> -	1	4	<i>m</i> -NHCOPr <sup>t</sup>	198 ± 64	6.70	16140	4.79

<sup>a</sup> K<sub>i</sub> ± SEM values were derived from 2–4 experiments performed in triplicate. <sup>b</sup> SEM is indicated when K<sub>i</sub> values were obtained from complete DRCs. <sup>c</sup> pK<sub>i</sub> values were calculated from K<sub>i</sub> values in M.

only one point of the curve was available was performed by the application of a method,<sup>7</sup> which consists of a simultaneous nonlinear regression analysis of all dose–response curves (DRCs) of the drug series using eq 1:

$$\% \text{ SB} = 100(1 - C_i^b / (\text{IC}_{50j}^b + C_i^b)) \quad (1)$$

where SB is the specific binding of radioligand, *b* is the slope, *i* = 1...*n* (measurements), and *j* = 1...*m* (number of compounds).

This analysis is performed under the assumption that all derivatives present the same mechanism of action within the given test model (i.e., parallel sigmoidal DRCs, identical Hill coefficients/slopes). This approach requires that complete DRCs (≥ 3 data pairs) are available for some analogues. Missing IC<sub>50</sub> values are obtained from “fragmentary” DRCs by a computational parallel shift of complete DRCs. IC<sub>50</sub> values were converted to K<sub>i</sub> values (Table 1) using the Cheng–Prusoff equation.<sup>8</sup>

Each chemical structure was described by six physicochemical parameters and three indicator variables. As electronic descriptors, the field and resonance constants of Swain and Lupton (*F*, *R*) were used. To attend a better quantification of the electrostatic effects, the *ortho*- and *meta*-position factors calculated by Williams and Norrington<sup>9</sup> were introduced. The van der Waals volumes (*V*<sub>o</sub>, *V*<sub>m</sub>) calculated with the SYBYL program<sup>10</sup> were employed as steric parameters. The hydrophobic effects exerted by the *ortho*- and *meta*-substituents were measured using Hansch π<sub>o</sub> and π<sub>m</sub> constants.<sup>11</sup>

**Table 2.** Indicator Variables and Physicochemical Parameters Used in the QSAR Study

compd	R	I <sub>A</sub>	I <sub>B</sub>	I <sub>n=3</sub>	F <sup>a</sup>	R <sup>a</sup>	V <sub>o</sub> <sup>b</sup>	V <sub>m</sub> <sup>b</sup>	π <sub>o</sub> <sup>c</sup>	π <sub>m</sub> <sup>c</sup>
1	<i>o</i> -OBu	0	0	1	0.513	-0.475	65.3	0.00	1.71	0.00
2	<i>o</i> -CONHPr	0	0	1	0.703	0.038	69.0	0.00	-0.09	0.00
3	<i>m</i> -NH <sub>2</sub>	0	0	1	0.036	-0.236	0.00	11.4	0.00	-1.23
4	<i>m</i> -Br	0	0	1	0.712	-0.061	0.00	17.2	0.00	0.86
5	<i>o</i> -CH <sub>3</sub>	1	0	1	-0.065	-0.122	16.4	0.00	0.56	0.00
6	<i>o</i> -COOPr	1	0	1	0.689	0.121	69.3	0.00	1.17	0.00
7	<i>o</i> -CN	1	0	1	1.057	0.159	15.9	0.00	-0.57	0.00
8	<i>m</i> -NHCOPr <sup>1</sup>	1	0	1	0.461	-0.095	0.00	70.8	0.00	0.11
9	<i>o</i> -CH <sub>3</sub>	0	1	1	-0.065	-0.122	16.4	0.00	0.56	0.00
10	<i>o</i> -COOPr	0	1	1	0.689	0.121	69.3	0.00	1.17	0.00
11	<i>o</i> -CN	0	1	1	1.057	0.159	15.9	0.00	-0.57	0.00
12	<i>m</i> -NHCOPr <sup>1</sup>	0	1	1	0.461	-0.095	0.00	70.8	0.00	0.11
13	<i>o</i> -OCH <sub>3</sub>	1	1	1	0.515	-0.431	22.7	0.00	-0.02	0.00
14	<i>o</i> -OBu	1	1	1	0.513	-0.475	65.3	0.00	1.71	0.00
15	<i>o</i> -CONHPr	1	1	1	0.703	0.038	69.0	0.00	-0.09	0.00
16	<i>m</i> -CF <sub>3</sub>	1	1	1	0.618	0.064	0.00	24.2	0.00	0.88
17	<i>o</i> -CH <sub>3</sub>	0	0	0	-0.065	-0.122	16.4	0.00	0.56	0.00
18	<i>o</i> -COOPr	0	0	0	0.689	0.121	69.3	0.00	1.17	0.00
19	<i>o</i> -CN	0	0	0	1.057	0.159	15.9	0.00	-0.57	0.00
20	<i>m</i> -NHCOPr <sup>1</sup>	0	0	0	0.461	-0.095	0.00	70.8	0.00	0.11
21	<i>o</i> -OBu	1	0	0	0.513	-0.475	65.3	0.00	1.71	0.00
22	<i>o</i> -CONHPr	1	0	0	0.703	0.038	69.0	0.00	-0.09	0.00
23	<i>m</i> -NH <sub>2</sub>	1	0	0	0.036	-0.236	0.00	11.4	0.00	-1.23
24	<i>m</i> -Br	1	0	0	0.712	-0.061	0.00	17.2	0.00	0.86
25	<i>o</i> -OCH <sub>3</sub>	0	1	0	0.515	-0.431	22.7	0.00	-0.02	0.00
26	<i>o</i> -OBu	0	1	0	0.513	-0.475	65.3	0.00	1.71	0.00
27	<i>o</i> -CONHPr	0	1	0	0.703	0.038	69.0	0.00	-0.09	0.00
28	<i>m</i> -CF <sub>3</sub>	0	1	0	0.618	0.064	0.00	24.2	0.00	0.88
29	<i>o</i> -CH <sub>3</sub>	1	1	0	-0.065	-0.122	16.4	0.00	0.56	0.00
30	<i>o</i> -COOPr	1	1	0	0.689	0.121	69.3	0.00	1.17	0.00
31	<i>o</i> -CN	1	1	0	1.057	0.159	15.9	0.00	-0.57	0.00
32	<i>m</i> -NHCOPr <sup>1</sup>	1	1	0	0.461	-0.095	0.00	70.8	0.00	0.11

<sup>a</sup> Data taken from ref 9. <sup>b</sup> Calculated with the SYBYL program. <sup>c</sup> Data taken from ref 11.

**Table 3.** Correlation Matrix for the Indicator Variables and Physicochemical Descriptors

	I <sub>A</sub>	I <sub>B</sub>	I <sub>n=3</sub>	F	R	V <sub>o</sub>	V <sub>m</sub>	π <sub>o</sub>	π <sub>m</sub>
I <sub>A</sub>	1								
I <sub>B</sub>	0	1							
I <sub>n=3</sub>	0	0	1						
F	0	0.075	0	1					
R	0	-0.021	0	0.480	1				
V <sub>o</sub>	0	0.048	0	0.243	-0.052	1			
V <sub>m</sub>	0	-0.012	0	-0.096	0.019	-0.547	1		
π <sub>o</sub>	0	-0.002	0	-0.316	-0.500	0.562	-0.238	1	
π <sub>m</sub>	0	0.180	0	0.366	0.232	-0.110	0.178	-0.048	1

The indicator variables I<sub>A</sub>, I<sub>B</sub> and I<sub>n=3</sub> indicate the presence or absence of certain structural elements: I<sub>A</sub> = 0 or 1 for X = -(CH<sub>2</sub>)<sub>3</sub>- or -(CH<sub>2</sub>)<sub>4</sub>-, I<sub>B</sub> = 0 or 1 for m = 0 or 1, and I<sub>n=3</sub> distinguishes between compounds where n = 3 (I<sub>n=3</sub> = 1) and n = 4 (I<sub>n=3</sub> = 0). The values of the input parameters as well as the intercorrelation among the physicochemical descriptors and the indicator variables are shown in Tables 2 and 3.

**Hansch Method.** A classical Hansch multivariate regression analysis using the least-squares method<sup>12</sup> was used to derive QSAR equations for our data set. The level of significance of each coefficient is judged by statistical procedures such as the Student *t* and *F* tests.<sup>13</sup>

To obtain suitable equations two factors must be taken into account. First, the ratio of compounds to variables should be greater than 5, and second, a minimal intercorrelation among the independent variables should be observed.

**ANN.** The neural network employed for this modeling was a fully connected three-layer network (input, hidden, output) trained by back-propagation (BP) of error.<sup>14</sup>

The hidden and output neurons received an additional constant input, the "bias". For the input layer a linear transfer function was used, and for the hidden and output layer the following sigmoid was taken, to enable modeling of nonlinear relations:

$$\text{out}_j = f(\text{net}_j) = 1/(1 + e^{-\text{net}_j}) \quad (2)$$

$$\text{net}_j = \sum_i (w_{ji} \text{out}_i) + \text{bias}_j \quad (3)$$

The input to neuron *j*, net<sub>*j*</sub>, is calculated by eq 3 where out<sub>*i*</sub> represents the output values from neurons *i* connected to *j*, w<sub>*ji*</sub> is the connection weight between neurons *i* and *j*, and bias<sub>*j*</sub> is the intercept of the linear combination  $\sum_i (w_{ji} \text{out}_i)$  which can be regarded as an extra weight of the neuron with a constant output of 1. Feedforward calculations and error BP were employed in this study. The BP algorithm is based on a gradient descent method to minimize an error function *E* with respect to the connection weights (w<sub>*ji*</sub>) and biases from the output layer toward the input layer. *E* is given as follows:

$$E = \sum_{i=1}^{i=N} \mathcal{E}_i^2 = \sum_{i=1}^{i=N} [y_i(\text{obsd}) - y_i(\text{cald})]^2 \quad (4)$$

where *N* is the number of objects in the training set,  $\mathcal{E}_i$  represents the error of the *i*th training data, y<sub>*i*</sub>(cald) is the calculated output value for the *i*th training data from the output neuron, and y<sub>*i*</sub>(obsd) is the observed value. Once the actual error produced by the network is known, partial derivatives of the error function are used to change the connection weights from their initially assigned random values according to the following equation:<sup>2</sup>

$$\Delta w_{ji}^l = \eta \delta_j^l \text{out}_i^{l-1} + \mu \Delta w_{ji}^{l(\text{previous})} \quad (5)$$

in which Δw<sub>*ji*</sub> denotes the applied adaptation of the weights from unit *i* to unit *j* in the next layer, δ<sub>*j*</sub><sup>*l*</sup> is the calculated correction factor of these weights, out<sub>*i*</sub> is the output of unit *i*, η is the learning rate, and μ is the momentum term. The learning rate, η, which determines the speed at which the weights change, is used to dampen the rate of change of the weights from iteration to iteration, whereas the momentum, μ, adds a certain amount of the weight change in the previous presentation to keep the direction of change from varying too fast, preventing possible oscillations.

The biological affinity (p*K*<sub>*i*</sub>) data set was scaled to lie in the range of -0.9 to +0.9, so as to allow margin for network predictions at the extremes. The input variables were scaled to lie in the range -0.75 to +0.75. The error BP was performed after each iteration. The networks were trained until no further significant change in the standard deviation, *s*, between observed and calculated affinities was observed. The optimal number of hidden neurons was determined by gradually eliminating nodes.<sup>15</sup> In all calculations random numbers in the range -0.1 to +0.1 were used to initialize the network weights. The momentum parameter was set at 0.7, while the learning rate was initially set at 0.1 and was reduced to 0.01 or 0.005 if oscillations in *s* were observed.

**Table 4.** Equations for QSAR of the 5-HT<sub>1A</sub> Serotonergic Receptor

equations <sup>a</sup>	<i>r</i>	SE	<i>F</i>
$pK_i = 7.66(\pm 0.18; 0.38; 42.5) - 0.251(\pm 0.114; 0.237; 2.19)I_A - 0.145(\pm 0.117; 0.244; 1.23)I_B - 0.762(\pm 0.114; 0.237; 6.64)I_{n=3} + 1.62(\pm 0.26; 0.54; 6.23)F + 0.078(\pm 0.353; 0.733; 0.221)R - 0.0284(\pm 0.0034; 0.0071; 8.24)V_o - 0.0195(\pm 0.0029; 0.0062; 6.53)V_m + 1.24(\pm 0.15; 0.31; 8.23)\pi_o + 0.136(\pm 0.160; 0.332; 0.848)\pi_m$ (6)	0.944	0.325	19.923
$pK_i = 7.65(\pm 0.17; 0.36; 45.0) - 0.251(\pm 0.112; 0.232; 2.23)I_A - 0.147(\pm 0.114; 0.237; 1.28)I_B - 0.762(\pm 0.114; 0.232; 6.78)I_{n=3} + 1.63(\pm 0.25; 0.52; 6.47)F - 0.0282(\pm 0.0033; 0.0068; 8.54)V_o - 0.0195(\pm 0.0029; 0.0060; 6.67)V_m + 1.22(\pm 0.13; 0.27; 9.24)\pi_o + 0.143(\pm 0.154; 0.318; 0.928)\pi_m$ (7)	0.944	0.318	23.374
$pK_i = 7.60(\pm 0.16; 0.34; 47.5) - 0.251(\pm 0.112; 0.231; 2.24)I_A - 0.128(\pm 0.112; 0.231; 1.14)I_B - 0.762(\pm 0.112; 0.231; 6.80)I_{n=3} + 1.74(\pm 0.21; 0.45; 8.00)F - 0.0292(\pm 0.0031; 0.0064; 9.30)V_o - 0.0192(\pm 0.0029; 0.0060; 6.63)V_m + 1.26(\pm 0.12; 0.25; 10.08)\pi_o$ (8)	0.941	0.317	26.743
$pK_i = 7.55(\pm 0.16; 0.33; 47.2) - 0.251(\pm 0.112; 0.232; 2.23)I_A - 0.762(\pm 0.112; 0.232; 6.76)I_{n=3} + 1.73(\pm 0.21; 0.45; 7.90)F - 0.0292(\pm 0.0031; 0.0065; 9.28)V_o - 0.0193(\pm 0.0029; 0.0060; 6.61)V_m + 1.26(\pm 0.12; 0.26; 10.02)\pi_o$ (9)	0.938	0.319	30.613

<sup>a</sup> *n* = 32.

**Molecular Model of the Complex between EF-7412 (33) and 5-HT<sub>1A</sub>R.** The 3D model of the transmembrane domain of the 5-HT<sub>1A</sub>R was constructed by computer-aided model building techniques from the crystal structure of RHO<sup>5</sup> (PDB access number 1F88). Conserved residues Asn 55 (residue number in the PDB file) or Asn 1.50 (nomenclature of Ballesteros & Weinstein),<sup>16</sup> Asp 83 or Asp 2.50, Arg 135 or Arg 3.50, Trp 161 or Trp 4.50, Pro 215 or Pro 5.50, Pro 267 or Pro 6.50, and Pro 303 or Pro 7.50 were employed in the alignment of RHO and human 5-HT<sub>1A</sub>R transmembrane sequences. The obtained molecular model was energy minimized (5000 steps), heated from 0 to 600 K in 30 ps, equilibrated from 30 to 150 ps at 600 K, cooled to 300 K from 150 to 210 ps, and equilibrated from 210 to 300 ps at 300 K. During these processes the C<sub>α</sub> atoms and the conserved residues were kept fixed at the positions originally determined in the crystal structure of RHO.<sup>5</sup> This procedure allows the arbitrarily positioned amino acid side chains to adopt an energetically favorable conformation.

The mode of recognition of the ligands was first determined by ab initio geometry optimization with the 3-21G\* basis set. The model system consisted on Asp 3.32 and Asn 7.39 (only the C<sub>α</sub> atom of the backbone is included) of the 5-HT<sub>1A</sub>R and the ligands pindolol (the indole ring and the terminal -CH(CH<sub>3</sub>)<sub>2</sub> were replaced by methyl groups) and EF-7412 (33) (the hydantoin moiety plus the -(CH<sub>2</sub>)<sub>4</sub>- chain were replaced by a methyl group). All free valences were capped with hydrogen atoms. The C<sub>α</sub> atoms of Asp 3.32 and Asn 7.39 were positioned and kept fixed at the positions previously obtained.<sup>5</sup> The optimized reduced model of the ligand-receptor complex was used to position the complete structure of EF-7412 (33) inside the previously equilibrated transmembrane domain of the 5-HT<sub>1A</sub>R. Subsequently, the complete system was energy minimized (5000 steps), heated (from 0 to 300 K in 15 ps) and equilibrated (from 15 to 500 ps). The geometries obtained during the trajectory from 400 to 500 ps (a total of 20) were averaged and energy minimized. The C<sub>α</sub> atoms were kept fixed at the positions originally determined<sup>5</sup> because of the absence of the lipid environment in the molecular dynamics simulations.

Quantum mechanical calculations were performed with the GAUSSIAN-98 system of programs.<sup>17</sup> Molecular dynamics simulations were run with the Sander module of AMBER5,<sup>18</sup> the all-atom force field,<sup>19</sup> SHAKE bond constraints in all bonds, a 2 fs integration time

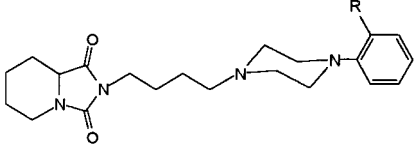
step, and a 13 Å cutoff for nonbonded interactions. Parameters for EF-7412 (33) were adapted from the Cornell et al. force field<sup>19</sup> using RESP point charges.<sup>20</sup>

## Results and Discussion

**Hansch Analysis. 5-HT<sub>1A</sub> Hansch Model:** Hansch equations for the serotonergic receptor were derived from multiple regression analysis between the pK<sub>i</sub> values at the 5-HT<sub>1A</sub> sites and the physicochemical parameters discussed in the Materials and Methods section. In eqs 6–9 reported in Table 4, *n* is the number of compounds, *r* is the correlation coefficient, SE is the standard error, and *F* is the value of the *F* test. The significance of each regression coefficient is expressed by its standard error, the partial correlation coefficient, and the Student *t*, all of them in parentheses. Analysis of the initial eq 6 reveals that *I*<sub>B</sub>, *R*, and *π*<sub>*m*</sub> are not statistically significant. The stepwise elimination of these descriptors from the analysis led to the eqs 7–9 in which electronic, steric, and hydrophobic effects are involved. Equation 9 was adopted as the final model, first because of its greater simplicity and second due to its satisfactory overall correlation.

Equation 9 shows that the structural features X = -(CH<sub>2</sub>)<sub>4</sub>- and especially *n* = 3 exert a negative effect on the affinity. High and positive values of *F* along with hydrophobic substituents at the *ortho*-position increase the 5-HT<sub>1A</sub> affinity. The above results also indicate that bulky substituents should be avoided for high affinity. Among the substituents that keep these requirements, we have selected *o*-Br and *o*-OPh in order to evaluate the predictive capacity of the model. Two new ligands, 34 and 35, were synthesized. The experimental and predicted values for both tested compounds are presented in Table 5, showing an acceptable overall agreement. The fact that the affinity of 35 is greater than expected for such a bulky substituent as the *o*-OPh indicates that the receptor is able to accommodate bulky substituents in this region of its active site.

**α<sub>1</sub> Hansch Model:** An approach identical to that used in the development of the QSAR for 5-HT<sub>1A</sub>R ligands was applied to the binding of the same ligands to the α<sub>1</sub>-adrenergic receptor, leading to the stepwise development of eqs 10–14 (Table 6). Following the same criteria as for the serotonergic receptor, eq 14 was selected as the best model. This equation indicates that the length of the alkyl chain seems to be irrelevant, while the presence of the hydantoin moiety exerts a

**Table 5.** Experimental and Predicted 5-HT<sub>1A</sub>  $K_i$  (eq 9) and  $\alpha_1$   $K_i$  (eq 14) Values of Compounds **34** and **35**


compd	R	F	$\pi_o$	$V_o$	5-HT <sub>1A</sub>		$\alpha_1$	
					$K_i$ exptl $\pm$ SEM (nM)	$K_i$ pred (nM)	$K_i$ exptl $\pm$ SEM (nM)	$K_i$ pred (nM)
<b>34</b>	<i>o</i> -Br	0.907	0.86	17.2	3.4 $\pm$ 0.6	0.4	6.2 $\pm$ 1.8	0.4
<b>35</b>	<i>o</i> -OPh	0.932	2.08	89.8	0.6 $\pm$ 0.2	1.2	2.4 $\pm$ 0.6	2.5

slightly positive effect at the  $\alpha_1$ -adrenergic active site. Electronic and hydrophobic requirements suggest that high and positive values of  $F$  as well as positive contributions of  $\pi$  at the *ortho*-position increase the  $\alpha_1$ -adrenergic receptor affinity. Equations 14 and 9 show that electronic and hydrophobic effects play a similar role in increasing affinity at both  $\alpha_1$ -adrenergic and 5-HT<sub>1A</sub> sites. With respect to the steric effects, bulky substituents decrease the affinity. However, it is interesting to note that negative steric effects are especially significant at the *meta*-position in eq 14, which indicates an important difference between the binding requirements at the 5-HT<sub>1A</sub> active site and the  $\alpha_1$ -adrenergic receptor. Thus, the *meta*-position seems to be implicated in the 5-HT<sub>1A</sub>/ $\alpha_1$  selectivity. Again, compounds **34** and **35** were used to investigate the predictive power of the derived model (Table 5).

Although the MLR studies conducted for the 5-HT<sub>1A</sub> and  $\alpha_1$ -adrenergic receptors have generated equations with an acceptable predictive power, it was desirable to investigate possible nonlinear relationships that may not be explained by the linear Hansch models.

**ANN Analysis. 5-HT<sub>1A</sub> ANN Model:** A three-layer BP learning network was used to study the set of 32 phenylpiperazines described above. The connection between the three different layers was complete. Initially the number of neurons in the input layer was equal to 9, identical to the number of molecular descriptors and indicator variables, whereas the output layer had only one neuron. The number of neurons in the hidden layer was determined by trial and error. The best correlation coefficient and lower standard deviation was obtained with three hidden layer neurons (9–3–1). The number of nodes in the hidden layer is an important factor determining the network's performance. It was found that too many nodes cause the network to memorize the data set (overfitting). However, networks with few nodes may be insufficient to use all the information of the data set (underfitting) and generalization is poor. It is desirable to establish a network which generalizes the input patterns rather than merely memorizing them. Previous studies conducted to determine the appropriate number of hidden units suggest that  $\rho$ , the ratio of the number of data points to the number of adjustable weights in the neural network, should have a value between 1.8 and 2.3.<sup>4,21</sup> For a network with a 9–3–1 configuration, the number of weights is 34, therefore  $\rho = 0.9$ , far from the optimal values. To reduce the complexity of the multilayer network and improve its ability to generalize, we have applied the 'forgetting' method<sup>22</sup> to the 9–3–1 network.

Using this technique, the weights are adjusted in a way that their differences are increased, allowing to distinguish which of them are less important and, therefore, to prune the corresponding input neuron. In Table 7 are shown the connection weights between the input layer and the hidden layer. As all inputs were scaled to an input range of  $-0.75$  to  $+0.75$ , the magnitude of the connection weights after training gave a direct indication of the contribution of each input parameter. Thus the input parameters with the smallest connection weights contributed least. To prune a given input parameter, the connections to the three hidden neurons should be small. Only two descriptors,  $R$  and  $\pi_m$ , fulfilled this condition. The elimination of two input neurons yields a 7–3–1 network with  $\rho = 1.1$ . This  $\rho$  value is still low, and for the final model an architecture of 7–2–1 was chosen with  $\rho = 1.7$ . Four sets of randomly assigned connection weights and biases were used to estimate the correlation coefficients corresponding to the global minimum of the network. For the final model  $r$ ,  $r^2$ , and  $s$  of the training set are 0.983, 0.966, and 0.149, respectively (Table 8).

To validate the model, the affinities for compounds **34** and **35** were predicted (Table 9). In light of these results, one can be confident that the neural network is able to provide reliable predictions of biological affinities of novel arylpiperazines.

**Dependence of Biological Activity on the Physicochemical Parameters:** The relative importance of each parameter in affecting the biological activity was investigated. It is known that the ANN model is difficult to interpret because it consists of some hidden nodes which produce nonlinear outputs for describing the nonlinear behavior in the data set. However, the variation of the affinity can be monitored in 3D diagrams by changing the values of two inputs while keeping the remaining inputs of the neural network constant at one-half of their maximum ranges. On the basis of the obtained plots, the 5-HT<sub>1A</sub> affinity seems to have a moderate nonlinear dependence on  $F$ ,  $V_o$ ,  $V_m$  and  $\pi_o$ , although the nonlinear relationship is not far from the planar one. This fact explains why the Hansch model shows an acceptable predictive power. It is interesting to note that the neural network is consistent with some of Hansch findings. First, both the neural network model and linear regression analysis agreed that positive values of  $F$  together with hydrophobic substituents at the *ortho*-position give high affinities, and second, bulky substituents exert a negative effect. The main discrepancy between the neural network model and the regression analysis seems to be the effect of  $I_B$ . While the size of the ring is irrelevant for the Hansch model, in the neural network model the highest values of affinity are observed for  $I_B = 0$ . These findings demonstrate that although the Hansch model is able to describe some features governing the 5-HT<sub>1A</sub> affinity, the ANN model reveals a certain nonlinear tendency, offering a better insight into the factors that are responsible for the serotonergic affinity and shows an enhanced predictive capacity.

**$\alpha_1$  ANN Model:** The same set of 32 phenylpiperazines was used to carry out this study. Initially a network with a configuration 9–3–1 was employed. The application of the forgetting effect led to the weights record in

**Table 6.** Equations for QSAR of the  $\alpha_1$ -Adrenergic Receptor

equations <sup>a</sup>	<i>r</i>	SE	<i>F</i>
$pK_i = 7.73(\pm 0.24; 0.51; 32.2) - 0.132(\pm 0.153; 0.318; 0.861)I_A - 0.321(\pm 0.157; 0.327; 2.03)I_B + 0.115(\pm 0.153; 0.318; 0.749)I_{R=3} + 1.14(\pm 0.34; 0.72; 3.26)F - 0.355(\pm 0.473; 0.982; 0.751)R - 0.0281(\pm 0.0046; 0.0095; 6.09)V_o - 0.0421(\pm 0.0040; 0.0083; 10.52)V_m + 1.03(\pm 0.20; 0.41; 5.11)\pi_o + 0.30(\pm 0.215; 0.446; 1.41)\pi_m$ (10)	0.933	0.435	16.528
$pK_i = 7.79(\pm 0.235; 0.486; 33.1) - 0.132(\pm 0.152; 0.315; 0.869)I_A - 0.321(\pm 0.156; 0.323; 2.05)I_B + 1.14(\pm 0.34; 0.71; 3.29)F - 0.355(\pm 0.469; 0.971; 0.758)R - 0.0281(\pm 0.0045; 0.0094; 6.15)V_o - 0.0421(\pm 0.0039; 0.0082; 10.62)V_m + 1.03(\pm 0.20; 0.41; 5.16)\pi_o + 0.304(\pm 0.213; 0.440; 1.42)\pi_m$ (11)	0.932	0.431	18.884
$pK_i = 7.84(\pm 0.22; 0.46; 35.6) - 0.132(\pm 0.150; 0.311; 0.877)I_A - 0.309(\pm 0.154; 0.318; 2.01)I_B + 1.101(\pm 0.33; 0.70; 3.24)F - 0.0288(\pm 0.0044; 0.0091; 6.48)V_o - 0.0422(\pm 0.0039; 0.0081; 10.72)V_m + 1.09(\pm 0.17; 0.36; 6.15)\pi_o + 0.272(\pm 0.207; 0.427; 1.31)\pi_m$ (12)	0.930	0.427	21.887
$pK_i = 7.77(\pm 0.21; 0.43; 36.7) - 0.309(\pm 0.153; 0.315; 2.01)I_B + 1.10(\pm 0.33; 0.69; 3.26)F - 0.0288(\pm 0.0044; 0.0091; 6.51)V_o - 0.0422(\pm 0.0039; 0.0080; 10.77)V_m + 1.09(\pm 0.17; 0.36; 6.18)\pi_o + 0.272(\pm 0.206; 0.424; 1.32)\pi_m$ (13)	0.927	0.425	25.644
$pK_i = 7.68(\pm 0.19; 0.41; 40.4) - 0.272(\pm 0.152; 0.314; 1.78)I_B + 1.32(\pm 0.29; 0.61; 4.44)F - 0.0306(\pm 0.0042; 0.0087; 7.16)V_o - 0.0417(\pm 0.0039; 0.0081; 10.54)V_m + 1.17(\pm 0.17; 0.35; 6.86)\pi_o$ (14)	0.922	0.431	29.570

<sup>a</sup> *n* = 32.**Table 7.** Values of the Connection Weights between the Input and Hidden Layers for the 5-HT<sub>1A</sub> ANN Model

	<i>N</i> <sub>1</sub>	<i>N</i> <sub>2</sub>	<i>N</i> <sub>3</sub>
<i>I</i> <sub>A</sub>	0.492	-0.744	-0.127
<i>I</i> <sub>B</sub>	-0.340	0.641	-0.549
<i>I</i> <sub>R=3</sub>	0.174	0.641	0.191
<i>F</i>	-0.612	-0.259	-0.041
<i>R</i>	0.045	-0.044	0.073
<i>V</i> <sub>o</sub>	-0.052	-0.048	-2.340
<i>V</i> <sub>m</sub>	0.479	0.229	-0.046
$\pi_o$	-0.633	-0.254	0.937
$\pi_m$	-0.280	-0.050	0.048
bias	0.355	1.251	2.017

**Table 8.** ANN Models

receptor	nonsignificant parameters	architecture	<i>r</i>	<i>r</i> <sup>2</sup>	<i>s</i>
5-HT <sub>1A</sub>	<i>R</i> , $\pi_m$	7-2-1	0.983	0.966	0.149
$\alpha_1$	<i>R</i>	8-2-1	0.991	0.982	0.136

**Table 9.** Experimental and Predicted *K*<sub>i</sub> Values by ANN Models of Compounds **34** and **35**

compd	5-HT <sub>1A</sub>		$\alpha_1$	
	<i>K</i> <sub>i</sub> exptl ± SEM (nM)	<i>K</i> <sub>i</sub> pred (nM)	<i>K</i> <sub>i</sub> exptl ± SEM (nM)	<i>K</i> <sub>i</sub> pred (nM)
<b>34</b>	3.4 ± 0.6	1.5	6.2 ± 1.8	3.2
<b>35</b>	0.6 ± 0.2	1.7	2.4 ± 0.6	7.2

**Table 10.** Values of the Connection Weights between the Input and Hidden Layers for the  $\alpha_1$  ANN Model

	<i>N</i> <sub>1</sub>	<i>N</i> <sub>2</sub>	<i>N</i> <sub>3</sub>
<i>I</i> <sub>A</sub>	-0.173	-0.246	-0.751
<i>I</i> <sub>B</sub>	0.049	0.553	1.867
<i>I</i> <sub>R=3</sub>	-0.094	0.609	0.733
<i>F</i>	0.328	0.292	-0.049
<i>R</i>	0.033	-0.278	0.045
<i>V</i> <sub>o</sub>	0.049	-1.526	0.030
<i>V</i> <sub>m</sub>	-0.456	-1.517	0.103
$\pi_o$	0.683	0.405	-0.072
$\pi_m$	-0.994	2.582	0.044
bias	0.313	0.047	1.642

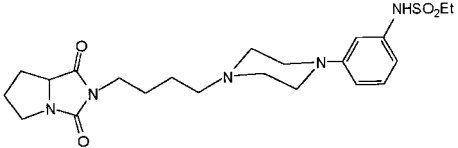
Table 10. In this case only one descriptor, *R*, could be eliminated, leading to the final architecture 8-2-1, with 21 connection weights and  $\rho = 1.5$ . The training process was repeated five times in order to find the global minimum of the network. For the final model *r*, *r*<sup>2</sup>, and *s* are 0.991, 0.982, and 0.136, respectively (Table 8). To investigate the predictive power of the derived

model, the affinities for compounds **34** and **35** were calculated (Table 9). A comparison of the observed and predicted values for both tested compounds shows a satisfactory agreement.

**Dependence of Biological Activity on the Physicochemical Parameters:** As for the 5-HT<sub>1A</sub>R, the variation of the affinity for the  $\alpha_1$ -adrenergic receptor was monitored in 3D diagrams by changing the values of two inputs while keeping the remaining ones at one-half of their maximum ranges. The obtained plots show a clear nonlinear dependence of the affinity on *F*, *V*<sub>o</sub>, *V*<sub>m</sub>,  $\pi_o$  and  $\pi_m$ . Moreover, the depicted surfaces do not appear to be simple mathematical functions. Nevertheless, the comparison of the Hansch analysis on this set of compounds with the ANN model shows certain similarities. For both models hydrophobic substituents at the *ortho*-position result in high activities, while bulky substituents at the *ortho* and especially at the *meta*-positions exert the opposite effect. The major difference between both models lies in the polar effects. In the Hansch correlation eq 14 high values of *F* strongly favor an increase in the predicted receptor affinity. 3D diagrams show clearly that an increase in the electronic parameter *F* exerts a detrimental effect on the affinity. A second difference was found on the lipophilicity of substituents at the *meta*-position. While in the Hansch model the hydrophobic properties of the groups at this position have no effect, in the ANN model high values of  $\pi_m$  were found to favor an increase in the predicted affinity. The explanation for these discrepancies between the neural network model and linear regression analysis seems to be the implicit nonlinear mapping performed by the neural network. Indeed the capability of the ANN to develop nonlinear terms underlines the strength of this approach and the improvements obtained.

#### Comparison of the 5-HT<sub>1A</sub> and $\alpha_1$ ANN Models.

A comparison of both analyses gives an additional understanding for the 5-HT<sub>1A</sub>/ $\alpha_1$  selectivity, leading to three important differences between both receptors. (a) Electrostatic factors: the polar factors are much more important for the 5-HT<sub>1A</sub>R than for the  $\alpha_1$ -adrenergic receptor. The serotonergic affinity increases with the increase of *F* values, while for the  $\alpha_1$ -adrenergic receptor the opposite effect was found. (b) Lipophilicity: hydrophobic substituents at the *ortho*-position result in high

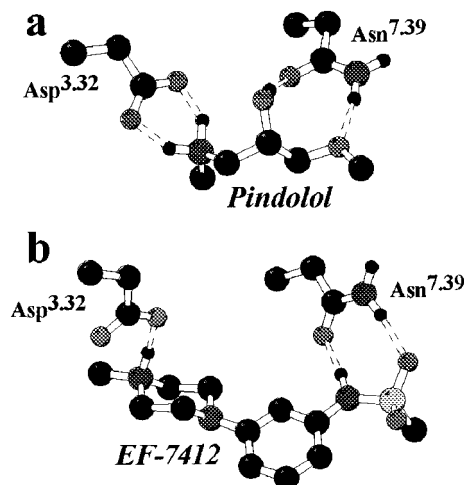
**Table 11.** Experimental and Predicted  $K_i$  Values for EF-7412 (**33**) According to Hansch and ANN Models at 5-HT<sub>1A</sub> and  $\alpha_1$ -Adrenergic Receptors


receptor	$K_i$ exptl $\pm$ SEM (nM)	$K_i$ pred (nM)	
		Hansch	ANN
5-HT <sub>1A</sub>	27 $\pm$ 8	98	36
$\alpha_1$	>1000	3158	2745

affinities, for both receptors. However, highly lipophilic groups at the *meta*-position only potentiate the affinity for the  $\alpha_1$ -adrenergic receptor. (c) Steric requirements at the *meta*-position: the *meta*-position seems to be significantly involved in the 5-HT<sub>1A</sub>/ $\alpha_1$  selectivity. While the 5-HT<sub>1A</sub>R is able to accommodate bulky substituents (about 60 Å<sup>3</sup>) in the region of its active site, the steric requirements of the  $\alpha_1$ -adrenergic receptor at this position are more restricted (between 0 and 22 Å<sup>3</sup>).

These results suggest that a good way to improve the 5-HT<sub>1A</sub>/ $\alpha_1$  selectivity would be the synthesis of long-chain derivatives ( $n = 4$ ) bearing a hydantoin moiety, according to the Hansch and ANN analysis, respectively. Both models reveal that the *meta*-position seems to be implicated in the 5-HT<sub>1A</sub>/ $\alpha_1$  selectivity. Thus bulky substituents with high  $F$  values and low  $\pi$  values would show an important selectivity for the 5-HT<sub>1A</sub>R. Among the different groups that fulfill these requirements *m*-NHSO<sub>2</sub>Et was chosen ( $F = 0.419$ ,  $\pi_m = -0.64$ ,  $V_m = 65.31$ ). On these bases, the new ligand EF-7412 (**33**) ( $X = -(CH_2)_3-$ ,  $m = 0$ ,  $n = 4$ ,  $R = m$ -NHSO<sub>2</sub>Et) was designed and synthesized. This analogue exhibits a high selectivity for the 5-HT<sub>1A</sub>R versus  $\alpha_1$ -adrenergic receptor ( $K_i = 27$  nM vs  $K_i > 1000$  nM) and also a satisfactory affinity. The Hansch and ANN predicted affinities for EF-7412 (**33**) are given in Table 11. These values clearly reveal the greater predictive power of the ANN model and the importance of the nonlinear relationships mapped by the neural network.

**Molecular Model of the Complex between EF-7412 (**33**) and 5-HT<sub>1A</sub>R.** In the preceding paper we reported the pharmacological characterization of EF-7412 (**33**) as an antagonist in vivo in pre- and postsynaptic 5-HT<sub>1A</sub>R sites. Mutagenesis experiments on GPCRs that bind protonated amine neurotransmitters indicate that the conserved Asp 3.32 is involved in the interaction with protonated amines of both agonists and antagonists (see ref 23 and references therein). Similarly, mutagenesis experiments on the  $\alpha_2$ <sup>24</sup>,  $\beta_2$ <sup>25</sup> and 5-HT<sub>1A</sub> receptors<sup>26</sup> have shown that the presence of an Asn residue at position 7.39 is important in conferring specificity to a series of ligands such as pindolol (PND) and propranolol. Moreover, the recognition of PND by Asn 7.39 occurs through two hydrogen bonds to the ether oxygen and the hydroxyl group of the ligand.<sup>27,28</sup> We can assume, as a working hypothesis, that EF-7412 (**33**) interacts with the 5-HT<sub>1A</sub>R sites in a similar manner throughout: (i) the ionic interaction between the protonated amine and Asp 3.32 and (ii) the hydrogen bonds between the *m*-NHSO<sub>2</sub>Et substituent and Asn 7.39. To identify the arrangement in space of these

**Figure 2.** Ab initio geometry optimization of the antagonist-binding site of the 5-HT<sub>1A</sub>R composed of the side chains of Asp 3.32 and Asn 7.39 (nomenclature of Ballesteros & Weinstein)<sup>16</sup> and (a) pindolol and (b) EF-7412 (**33**). Nonpolar hydrogens are not depicted to offer a better view of the recognition pocket.

essential determinants for recognition, we performed ab initio geometry optimization of PND and EF-7412 (**33**) inside the side chains of Asp 3.32 and Asn 7.39 (see Materials and Methods for computational details).

Figure 2 presents a detailed view of Asp 3.32 and Asn 7.39 in its interaction with PND (Figure 2a) and EF-7412 (**33**) (Figure 2b). The ionic interaction between the protonated amine of PND and Asp 3.32 occurs through the two N-H groups pointing toward both O <sub>$\delta$</sub>  atoms of Asp at optimized distances between heteroatoms of 2.58 and 2.54 Å (see Figure 2a). Similarly, the unique N-H group of the protonated amine of EF-7412 (**33**) interacts with one of the O <sub>$\delta$</sub>  atoms of Asp at an optimized distance between heteroatoms of 2.51 Å (see Figure 2b). The recognition of PND by Asn 7.39<sup>27,28</sup> occurs through hydrogen bonds between the ether oxygen and the hydroxyl group of PND and the N-H and C=O groups of Asn, at optimized distances between heteroatoms of 2.84 and 2.75 Å, respectively. The *m*-NHSO<sub>2</sub>Et group of EF-7412 (**33**) can fulfill a similar hydrogen bond network (see Figure 2b). The N-H group of the *m*-NHSO<sub>2</sub>Et substituent acts as a hydrogen bond donor in the hydrogen bond interaction with the C=O group of Asn (2.72 Å), whereas the S=O group acts as a hydrogen bond acceptor in the hydrogen bond with the N-H group of Asn (2.89 Å). It is important to remark that although the ether oxygen and the hydroxyl group of PND and the *m*-NHSO<sub>2</sub>Et group of EF-7412 (**33**) are structurally dissimilar, these are interacting in a similar manner with Asn 7.39 and thus serving an analogous function. Moreover, the absence of Asn 7.39 in the  $\alpha_1$ -adrenergic receptor explains the selectivity of EF-7412 (**33**) for the 5-HT<sub>1A</sub>R sites.

The obtained complex depicted in Figure 2b between the modeled part of EF-7412 (**33**) and Asp 3.32 and Asn 7.39 was used to position the complete structure of EF-7412 (**33**) inside a 3D model of the transmembrane domain of the 5-HT<sub>1A</sub>R (see Materials and Methods for computational details). Figure 3 shows EF-7412 (**33**) in the binding pocket of the 5-HT<sub>1A</sub>R, in a view perpendicular (Figure 3a) and parallel (Figure 3b) to the membrane. Figure 3c presents a detailed view of the

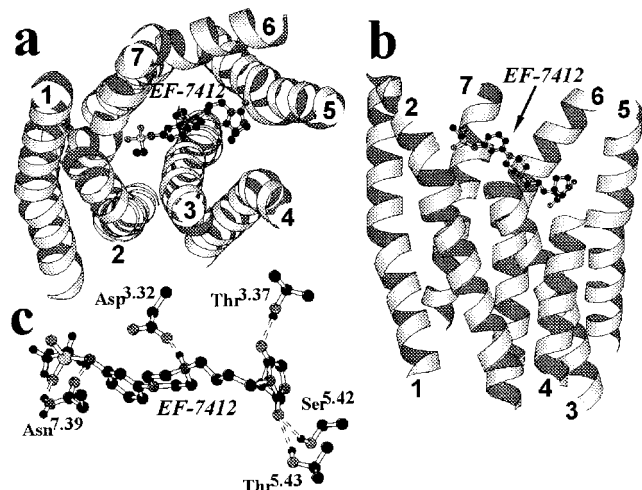


**Figure 3.** Molecular model of the transmembrane helix bundle of the 5-HT<sub>1A</sub>R constructed from the crystal structure of bovine rhodopsin.<sup>5</sup> EF-7412 (**33**) is shown in the binding pocket (a) in a view perpendicular to the membrane, (b) in a view parallel to the membrane, and (c) in a detailed view of the ligand-binding site. The binding mode includes: (i) ionic interaction between the protonated amine of the ligand and Asp 3.32; (ii) hydrogen bonds between the *m*-NHSO<sub>2</sub>Et group of the ligand and Asn 7.39; and hydrogen bonds between the hydantoin moiety of the ligand and (iii) Thr 3.37, (iv) Ser 5.42, and (v) Thr 5.43 (nomenclature of Ballesteros & Weinstein).<sup>16</sup> Nonpolar hydrogens are not depicted to offer a better view of the recognition pocket. Figure was created using MOLSCRIPT.<sup>38</sup>

ligand-binding site. The proposed recognition of the endogenous ligand involves, in addition to the (i) ionic and (ii) hydrogen bond interactions with Asp 3.32 and Asn 7.39 (see above), the hydrogen bonds between both C=O groups of the hydantoin moiety of the ligand and (iii) Thr 3.37 (3.06 Å), (iv) Ser 5.42 (3.42 Å), and (v) Thr 5.43 (3.70 Å) of the 5-HT<sub>1A</sub>R. Mutation of Thr 3.37 to Ala in the  $\alpha_{1B}$  receptor<sup>29</sup> decreases the affinity of the antagonist prazosin by a factor of 6. This result indicates that this locus is approachable by the extracellular ligand. On the other hand, mutagenesis experiments have shown that a series of conserved Ser or Thr residues at positions 5.42 and 5.43 act as hydrogen-bonding sites for the hydroxyl groups present in the chemical structure of many neurotransmitters and synthetic agonists (see ref 23 and references therein). In particular, Ser 5.42 and Thr 5.43 are important in the binding of 5-HT to the 5-HT<sub>1A</sub>R.<sup>30</sup> Thus, Asp 3.32, Ser 5.42, and Thr 5.43 are common anchoring residues of both agonists and EF-7412 (**33**). We can conclude that EF-7412 (**33**) binds to the same receptor sites than agonists do and act by blocking the access of agonists to receptor sites.

## Conclusion

A classical QSAR and ANN analysis have been successfully applied to a series of 32 phenylpiperazines with affinity for 5-HT<sub>1A</sub> and  $\alpha_1$ -adrenergic receptors. The resulting models provide a significant correlation of electrostatic, steric, and lipophilic parameters with biological affinities. Although the derived linear Hansch models are able to give acceptable predictions, the introduction of nonlinear relationships in the analysis clearly gives more solid models and more accurate

predictions. The obtained Hansch and ANN models for the 5-HT<sub>1A</sub> and  $\alpha_1$ -adrenergic receptors led us to design and synthesize a new antagonist, EF-7412 (**33**), with a high selectivity profile for the 5-HT<sub>1A</sub>R sites. The computed model of the complex between EF-7412 (**33**) and a 3D structure of the transmembrane domain of the 5-HT<sub>1A</sub>R has identified the key structural features of both EF-7412 (**33**) and the 5-HT<sub>1A</sub>R that are responsible for complex formation. Classical Hansch analysis, ANNs, and the detailed 3D model of the ligand–receptor complex provide an essential tool for the development of highly desirable,<sup>31</sup> selective 5-HT<sub>1A</sub> antagonists.

## Experimental Section

**Chemistry.** Melting points (uncorrected) were determined on a Gallenkamp electrothermal apparatus. Infrared (IR) spectra were obtained on a Perkin-Elmer 781 infrared spectrophotometer. <sup>1</sup>H and <sup>13</sup>C NMR spectra were recorded on a Varian VXR-300S or Bruker 250-AM instrument. Chemical shifts ( $\delta$ ) are expressed in parts per million relative to internal tetramethylsilane; coupling constants (*J*) are in hertz (Hz). Elemental analyses (C, H, N) were determined within 0.4% of the theoretical values. Thin-layer chromatography (TLC) was run on Merck silica gel 60 F-254 plates. For normal pressure and flash chromatography, Merck silica gel type 60 (size 70–230 and 230–400 mesh, respectively) was used. Unless stated otherwise, starting materials used were high-grade commercial products.

The 2-(4-bromobutyl)-1,3-dioxoperhydroimidazo[1,5-*a*]pyridine was synthesized according to the literature.<sup>32</sup> 1-Arylpiperazines were prepared by reaction of the corresponding anilines with bis(2-chloroethyl)amine, as previously described.<sup>33,34</sup>

**2-[4-[4-(*o*-Bromophenyl)piperazin-1-yl]butyl]- and 2-[4-[4-(*o*-(Phenoxy)phenyl)piperazin-1-yl]butyl]-1,3-dioxoperhydroimidazo[1,5-*a*]pyridine (**34**, **35**). **General Procedure.** To a suspension of 2-(4-bromobutyl)-1,3-dioxoperhydroimidazo[1,5-*a*]pyridine (9 mmol) and the corresponding 1-arylpiperazine (15 mmol) in acetonitrile (20 mL), was added 2.0 mL of triethylamine (1.5 g, 14.6 mmol). The mixture was refluxed for 20–24 h. Then, the solvent was evaporated under reduced pressure and the residue was resuspended in water and extracted with dichloromethane (3 × 100 mL). The combined organic layers were washed with water and dried over MgSO<sub>4</sub>. After evaporation of the solvent the crude oil was purified by column chromatography (eluents: ethyl acetate/ethanol 9:1). Spectral data refer to the free base and then hydrochloride salts were prepared.**

**2-[4-[4-(*o*-Bromophenyl)piperazin-1-yl]butyl]-1,3-dioxoperhydroimidazo[1,5-*a*]pyridine (**34**):** yield 56%; mp 220–222 °C (methanol/ethyl ether); <sup>1</sup>H NMR (CDCl<sub>3</sub>)  $\delta$  1.22–1.69 (m, 8H), 1.92 (dm, *J* = 13.5, 1H), 2.14 (dd, *J* = 13.2, 3.6, 1H), 2.36 (t, 2H), 2.56 (brs, 4H), 2.76 (td, *J* = 12.3, 3.6, 1H), 3.00 (brs, 4H), 3.46 (t, *J* = 7.2, 2H), 3.67 (dd, *J* = 12.0, 4.2, 1H), 4.10 (dd, *J* = 13.5, 4.8, 1H), 6.83 (td, *J* = 8.1, 1.5, 1H), 6.98 (dd, *J* = 7.8, 1.5, 1H), 7.19 (td, *J* = 7.8, 1.5, 1H), 7.48 (dd, *J* = 8.1, 1.5, 1H); <sup>13</sup>C NMR (CDCl<sub>3</sub>)  $\delta$  22.7, 24.0, 24.9, 26.2, 27.8, 38.5, 39.2, 51.6, 53.3, 57.2, 58.0, 119.8, 120.8, 124.2, 128.2, 133.7, 150.6, 154.4, 173.1. Anal. (C<sub>21</sub>H<sub>29</sub>BrN<sub>4</sub>O<sub>2</sub>·HCl) C, H, N.

**2-[4-[4-(*o*-(Phenoxy)phenyl)piperazin-1-yl]butyl]-1,3-dioxoperhydroimidazo[1,5-*a*]pyridine (**35**):** yield 64%; mp 171–173 °C (methanol/ethyl ether); <sup>1</sup>H NMR (CDCl<sub>3</sub>)  $\delta$  1.23–1.65 (m, 7H), 1.73 (d, *J* = 10.8, 1H), 1.98 (dm, *J* = 12.3, 1H), 2.19 (dd, *J* = 9.8, 3.8, 1H), 2.38 (tt, *J* = 7.5, 2H), 2.49 (brs, 4H), 2.82 (td, *J* = 12.6, 3.6, 1H), 3.15 (brs, 4H), 3.50 (t, *J* = 6.9, 2H), 3.73 (dd, *J* = 11.7, 3.9, 1H), 4.15 (dd, *J* = 14.7, 3.0, 1H), 6.91–7.12 (m, 7H), 7.28 (dd, *J* = 8.4, 7.5, 2H); <sup>13</sup>C NMR (CDCl<sub>3</sub>)  $\delta$  22.7, 23.5, 24.9, 26.0, 27.7, 38.3, 39.2, 49.8, 53.1, 57.2, 57.8, 117.2, 119.1, 121.1, 122.3, 122.7, 124.6, 129.3, 143.6, 148.5, 154.4, 157.3, 173.1. Anal. (C<sub>27</sub>H<sub>34</sub>N<sub>4</sub>O<sub>3</sub>·2HCl·2H<sub>2</sub>O) C, H, N.

**Radioligand Binding Assays.** For all receptor binding assays, male Sprague–Dawley rats (*Rattus norvegicus albi*–



nus), weighing 180–200 g, were killed by decapitation and the brains rapidly removed and dissected.

**5-HT<sub>1A</sub> Receptor.** The receptor binding studies were performed by a modification of a previously described procedure.<sup>35</sup> The cerebral cortex was homogenized in 10 volumes of ice-cold Tris buffer (50 mM Tris-HCl, pH 7.7 at 25 °C) and centrifuged at 28000g for 15 min. The membrane pellet was washed twice by resuspension and centrifugation. After the second wash the resuspended pellet was incubated at 37 °C for 10 min. Membranes were then collected by centrifugation and the final pellet was resuspended in 50 mM Tris-HCl, 5 mM MgSO<sub>4</sub>, and 0.5 mM EDTA buffer (pH 7.4 at 37 °C). Fractions of the final membrane suspension (about 1 mg of protein) were incubated at 37 °C for 15 min with 0.6 nM [<sup>3</sup>H]-8-OH-DPAT (8-hydroxy-2-(dipropylamino)tetralin) (133 Ci/mmol), in the presence or absence of several concentrations of the competing drug, in a final volume of 1.1 mL of assay buffer (50 mM Tris-HCl, 10 nM clonidine, 30 nM prazosin, pH 7.4 at 37 °C). Nonspecific binding was determined with 10 μM 5-HT.

**α<sub>1</sub>-Adrenergic Receptor.** The radioligand receptor binding studies were performed according to a previously described procedure.<sup>36</sup> The cerebral cortex was homogenized in 20 volumes of ice-cold buffer (50 mM Tris-HCl, 10 mM MgCl<sub>2</sub>, pH 7.4 at 25 °C) and centrifuged at 30000g for 15 min. Pellets were washed twice by resuspension and centrifugation. Final pellets were resuspended in the same buffer. Fractions of the final membrane suspension (about 250 μg of protein) were incubated at 25 °C for 30 min with 0.2 nM [<sup>3</sup>H]prazosin (23 Ci/mmol) in the presence or absence of several concentrations of the competing drug, in a final volume of 2 mL of buffer. Nonspecific binding was determined with 10 μM phentolamine.

For all binding assays, competing drug, nonspecific, total and radioligand bindings were defined in triplicate. Incubation was terminated by rapid vacuum filtration through Whatman GF/B filters, presoaked in 0.05% poly(ethylenimine), using a Brandel cell harvester. The filters were then washed with the assay buffer and dried. The filters were placed in poly(ethylene) vials to which were added 4 mL of a scintillation cocktail (Aquasol), and the radioactivity bound to the filters was measured by liquid scintillation spectrometry. The data were analyzed by an iterative curve-fitting procedure (program Prism, Graph Pad), which provided IC<sub>50</sub>, K<sub>i</sub>, and r<sup>2</sup> values for test compounds, K<sub>i</sub> values being calculated from the Cheng and Prusoff equation.<sup>8</sup> The protein concentrations of the rat cerebral cortex and the rat striatum were determined by the method of Lowry,<sup>37</sup> using bovine serum albumin as the standard.

**Acknowledgment.** This work was supported by grants from DGESIC (PB97-0282), CICYT (SAF99-073), Comunidad de Madrid (08.5/000466.1/98), and Fundació La Marató TV3 (0014/97). Some of the simulations were run at the Centre de Computació i Comunicacions de Catalunya. The authors are grateful to UNED for a predoctoral grant to E.F. and the German Academic Exchange Service (DAAD) for financial support of M.L.R. in the form of a 10-month research stipend.

**Supporting Information Available:** 3D diagrams of ANN models. This information is available free of charge via the Internet at <http://pubs.acs.org>.

## References

- (1) (a) Hansch, C.; Fujita, T.  $\rho$ - $\sigma$ - $\pi$  Analysis. A Method for the Correlation of Biological Activity and Chemical Structure. *J. Am. Chem. Soc.* **1964**, *86*, 1616–1626. (b) Kubiny, H. QSAR: Hansch Analysis and Related Approaches. In *Methods and Principles in Medicinal Chemistry*; VCH: Weinheim, New York, 1993; Vol. I.
- (2) Zupan, J.; Gasteiger, J. *Neural Networks for Chemists: An Introduction*; VCH: New York, 1993.
- (3) Devillers, J., Ed. *Neural Networks in QSAR and Drug Design*. In *Principles of QSAR and Drug Design*; Academic Press: London, 1996.
- (4) Andrea, T. A.; Kalayeh, H. Applications of Neural Networks in Quantitative Structure–Activity Relationships of Dihydrofolate Reductase Inhibitors. *J. Med. Chem.* **1991**, *34*, 2824–2836.
- (5) Palczewski, K.; Kumasaka, T.; Hori, T.; Behnke, C. A.; Motoshima, H.; Fox, B. A.; Trong, I. L.; Teller, D. C.; Okada, T.; Stenkamp, R. E.; Yamamoto, M.; Miyano, M. Crystal Structure of Rhodopsin: A G Protein-coupled Receptor. *Science* **2000**, *289*, 739–745.
- (6) Bourne, H. R.; Meng, E. C. Rhodopsin Sees the Light. *Science* **2000**, *289*, 733–734.
- (7) Schaper, K.-J.; Emig, P.; Engel, J.; Fleischhauer, I.; Kutscher, B.; Rosado, M. L.; López-Rodríguez, M. L. Dose Response Relationships, Biotest Intercorrelations, QSAR and the Saving of Animals Experiments. In *QSAR and Molecular Modelling: Concepts, Computational Tools and Biological Applications*; Sanz, F., Giraldo, J., Manaut, F., Eds.; Prous Science: Barcelona, 1995; pp 73–76.
- (8) Cheng, Y. C.; Prusoff, W. H. Relationship between the Inhibition Constant (K<sub>i</sub>) and the Concentration of Inhibitor which Causes 50 Per Cent Inhibition (IC<sub>50</sub>) of an Enzymatic Reaction. *Biochem. Pharmacol.* **1973**, *22*, 3099–3108.
- (9) Williams, S. G.; Norrington, F. E. Determination of Positional Weighting Factors for the Swain and Lupton Substituent Constants  $\rho$  and  $\sigma$ . *J. Am. Chem. Soc.* **1976**, *98*, 508–516.
- (10) SYBYL Molecular Modelling System (version 6.0), Tripos Associates, 1699 S. Hanley Rd., St. Louis, MO 63144.
- (11) Hansch, C.; Leo, A. J.; Hoekman, D. *Exploring QSAR: Hydrophobic, Electronic and Steric Constants*; ACS Professional Reference Book, ACS Advisory Board: Washington, D.C., 1995.
- (12) Hansch, C. In *Structure–Activity Relationships*; Cavallito, C. J., Ed.; Pergamon Press: Oxford, 1973; Vol. 1, p 50.
- (13) Bennet, C. A.; Franklin, N. L. *Statistical Analysis in Chemistry and the Chemical Industry*; Wiley: New York, 1963.
- (14) Rumelhart, D. E.; Hinton, G. E.; Williams, R. J. Learning Representations by Back-propagating Errors. *Nature* **1986**, *323*, 533–536.
- (15) Schaper, K.-J. Free-Wilson-Type Analysis of Non-Additive Substituent Effects on THPB Dopamine Receptor Affinity Using Artificial Neural Networks. *Quant. Struct.-Act. Relat.* **1999**, *18*, 354–360.
- (16) Ballesteros, J. A.; Weinstein, H. Integrated Methods for the Construction of Three-Dimensional Models and Computational Probing of Structure–function Relations in G-Protein Coupled Receptors. *Methods Neurosci.* **1995**, *25*, 366–428.
- (17) Frisch, M. J.; Trucks, G. W.; Schlegel, H. B.; Scuseria, G. E.; Robb, M. A.; Cheeseman, J. R.; Zakrzewski, V. G.; Montgomery, J. A.; Keith, T. A.; Petersson, G. A.; Raghavachari, K.; Al-Laham, A.; Stratmann, R. E.; Burant, J. C.; Dapprich, S.; Millam, J. M.; Daniels, A. D.; Kudin, K. N.; Strain, M. C.; Farkas, O.; Tomasi, J.; Barone, V.; Cossi, M.; Cammi, R.; Mennucci, B.; Pomelli, C.; Adamo, C.; Clifford, S.; Ochterski, J.; Petersson, G. A.; Ayala, P. Y.; Cui, Q.; Morokuma, K.; Malick, D. K.; Rabuck, A. D.; Raghavachari, K.; Foresman, J. B.; Cioslowski, J.; Ortiz, J. V.; Stefanov, B. B.; Liu, G.; Liashenko, A.; Piskorz, P.; Komaromi, I.; Gomperts, R.; Martin, R. L.; Fox, D. J.; Keith, T.; Al-Laham, M. A.; Peng, C. Y.; Nanayakkara, A.; González, C.; Challacombe, M.; Gill, P. M. W.; Johnson, B. G.; Chen, W.; Wong, W.; Andres, J. L.; HeadBGordon, M.; Replogle, E. S.; Pople, J. A. Gaussian 98; Gaussian Inc., Pittsburgh, PA.
- (18) Case, D. A.; Pearlman, D. A.; Caldwell, J. W.; Cheatham, III, T. E.; Ross, W. S.; Simmerling, C. L.; Darden, T. A.; Merz, K. M.; Stanton, R. V.; Cheng, A. L.; Vicent, J. J.; Crowley, M.; Ferguson, D. M.; Radmer, R. J.; Seibel, G. L.; Singh, U. C.; Weiner, P. K.; Kollman, P. A. AMBER 5; University of California, San Francisco, 1997.
- (19) Cornell, W. D.; Cieplak, P.; Bayly, C. I.; Gould, I. R.; Merz, Jr., K. M.; Ferguson, D. M.; Spellmeyer, D. C.; Fox, T.; Caldwell, J. W.; Kollman, P. A. A Second Generation Force Field for the Simulation of Proteins, Nucleic Acids, and Organic Molecules. *J. Am. Chem. Soc.* **1995**, *117*, 5179–5197.
- (20) Cieplak, P.; Cornell, W. D.; Bayly, C.; Kollman, P. A. Application of the Multimolecule and Multiconformational RESP Methodology to Biopolymers: Charge Derivation for DNA, RNA and Proteins. *J. Comput. Chem.* **1995**, *16*, 1357–1377.
- (21) So, S. S.; Richards, W. G. Application of Neural Networks: Quantitative Structure–Activity Relationships of the Derivatives of 2,4-Diamino-5-(substituted-benzyl)pyrimidines as DHFR Inhibitors. *J. Med. Chem.* **1992**, *35*, 3201–3207.
- (22) Aoyama, T.; Ichikawa, H. Reconstruction of Weight Matrixes in Neural Networks—a Method of Correlating Outputs with Inputs. *Chem. Pharm. Bull.* **1991**, *39*, 1222–1228.
- (23) Rhee, A. M.; Jacobson, K. A. Molecular Architecture of G Protein-Coupled Receptors. *Drug Dev. Res.* **1996**, *37*, 1–38.
- (24) Suryanarayana, S.; Daunt, D. A.; Zastrow, M. V.; Kobilka, B. K. A Point Mutation in the Seventh Hydrophobic Domain of the α<sub>2</sub>-Adrenergic Receptor Increases its Affinity for a Family of β-Receptor Antagonists. *J. Biol. Chem.* **1991**, *266*, 15488–15492.

- (25) Suryanarayana, S.; Kobilka, B. K. Amino Acid Substitutions at Position 312 in the Seventh Hydrophobic Segment of the  $\beta_2$ -Adrenergic Receptor Modify Ligand-Binding Specificity. *Mol. Pharmacol.* **1993**, *44*, 111–114.
- (26) Guan, X.-M.; Peroutka, S. J.; Kobilka, B. K. Identification of a Single Amino Acid Residue Responsible for the Binding of a Class of Beta-Adrenergic Receptor Antagonists to 5-HT<sub>1A</sub> Receptors. *Mol. Pharmacol.* **1992**, *41*, 695–698.
- (27) Glennon, R. A.; Dukat, M.; Westkaemper, R. B.; Ismaiel, A. M.; Izzarelli, D. G.; Parker, E. M. The Binding of Propranolol at 5-Hydroxytryptamine<sub>1D $\beta$</sub>  T355N Mutant Receptors May Involve Formation of Two Hydrogen Bonds to Asparagine. *Mol. Pharmacol.* **1996**, *49*, 198–206.
- (28) Pardo, L.; Batlle, M.; Duñach, M.; Weinstein, H. The Structure and Activity of Membrane Receptors: Modeling and Computational Simulation of Ligand Recognition in a Three-Dimensional Model of the 5-Hydroxytryptamine<sub>1A</sub> Receptor. *J. Biomed. Sci.* **1996**, *3*, 98–107.
- (29) Cavalli, A.; Fanelli, F.; Taddei, C.; De Benedetti, P. G.; Cotecchia, S. Amino Acids of the Alpha<sub>1 $\beta$</sub> -Adrenergic Receptor Involved in Agonist Binding: Differences in Docking Catecholamines to Receptor Subtypes. *FEBS Lett.* **1996**, *399*, 9–13.
- (30) Ho, B. Y.; Karschin, A.; Branchek, T.; Davidson, N.; Lester, H. A. The Role of Conserved Aspartate and Serine Residues in Ligand Binding and in Function of the 5-HT<sub>1A</sub> Receptor: A Site-directed Mutation Study. *FEBS Lett.* **1992**, *312*, 259–262.
- (31) Fletcher, A.; Cliffe, I. A.; Dourish, C. T. Silent 5-HT<sub>1A</sub> Receptor Antagonists: Utility as Research Tools and Therapeutic Agents. *Trends Pharmacol. Sci.* **1993**, *14*, 441–448.
- (32) López-Rodríguez, M. L.; Rosado, M. L.; Benhamú, B.; Morcillo, M. J.; Sanz, A. M.; Orensanz, L.; Beneytez, M. E.; Fuentes, J. A.; Manzanares, J. Synthesis and Structure–Activity Relationships of a New Model of Arylpiperazines. 1. 2-[[4-(*o*-Methoxyphenyl)piperazin-1-yl]methyl]-1,3-dioxoperhydroimidazo[1,5-*a*]pyridine: A Selective 5-HT<sub>1A</sub> Receptor Agonist. *J. Med. Chem.* **1996**, *39*, 4439–4450.
- (33) Lyon, R. A.; Titeler, M.; McKenney, J. D.; Magee, P. S.; Glennon, R. A. Synthesis and Evaluation of Phenyl- and Benzoylpiperazines as Potential Serotonergic Agents. *J. Med. Chem.* **1986**, *29*, 630–634.
- (34) Martin, G. E.; Elgin, R. J., Jr.; Mathiasen, J. R.; Davis, C. B.; Kesslick, J. M.; Baldy, W. J.; Shank, R. P.; DiStefano, D. L.; Fedde, C. L.; Scott, M. K. Activity of Aromatic Substituted Phenylpiperazines Lacking Affinity for Dopamine Binding Sites in a Preclinical Test of Antipsychotic Efficacy. *J. Med. Chem.* **1989**, *32*, 1052–1056.
- (35) Clark, R. D.; Weinhardt, K. K.; Berger, J.; Fischer, L. E.; Brown, C. M.; MacKinnon, A. C.; Kilpatrick, A. T.; Spedding, M. 1,9-Alkano-bridged 2,3,4,5-Tetrahydro-1*H*-3-benzazepines with Affinity for the  $\alpha_2$ -Adrenoceptor and the 5-HT<sub>1A</sub> Receptor. *J. Med. Chem.* **1990**, *33*, 633–641.
- (36) Ambrosio, E.; Montero, M. T.; Fernández, I.; Azuara, M. C.; Orensanz, L. M. [<sup>3</sup>H]Prazosin Binding to Central Nervous System Regions of Male and Female Rats. *Neurosci. Lett.* **1984**, *49*, 193–197.
- (37) Lowry, O. H.; Rosebrough, N. J.; Farr, A. L.; Randall, R. J. Protein Measurement with the Folin Phenol Reagent. *J. Biol. Chem.* **1951**, *193*, 265–275.
- (38) Kraulis, J. MOLSCRIPT: A Program to Produce Both Detailed and Schematic Plots of Protein Structure. *J. Appl. Crystallogr.* **1991**, *24*, 946–950.

JM000930T